

Heterozygous mutation of *SLC34A1* in patients with hypophosphatemic kidney stones and osteoporosis: a case report

Journal of International Medical Research
48(3) 1–8

© The Author(s) 2020

Article reuse guidelines:

sagepub.com/journals-permissions

DOI: 10.1177/0300060519896146

journals.sagepub.com/home/imr



Yuping Ma, Haihong Lv , Jue Wang and
Jiaojiao Tan

Abstract

Hypophosphatemic kidney stones with osteoporosis is a rare disease clinically. Mutations in the solute carrier family 34 member 1 gene (*SLC34A1*), encoding NaPi-IIa, are considered to be associated with this disease. In this report, a 38-year-old Chinese woman was diagnosed with hypophosphatemic kidney stones with osteoporosis. Her clinical features were recorded, and biochemical tests and DNA sequencing were performed of the proband and her parents. Sequencing revealed that she inherited the c.1753T>C *SLC34A1* mutation from her mother. This mutation in exon 13 of *SLC34A1* causes a substitution of serine with proline (p. S585P) at position 585 of NaPi-IIa. This is a novel mutation that has not previously been reported, and which shows autosomal dominant inheritance. It is expected to lead to changes in protein function, and we believe that it is the cause of pathology in our patient.

Keywords

NaPi-IIa, hypophosphatemic kidney stones, *SLC34A1*, DNA sequencing, point mutation, osteoporosis

Date received: 23 August 2019; accepted: 29 November 2019

Introduction

Inorganic phosphates are involved in a wide range of cellular processes, including intracellular signal transduction, energy exchange, pH buffering, bone mineralization, cellular

Department of Endocrinology and Metabolism, The First Hospital of Lanzhou University, Lanzhou, Gansu, P.R. China

Corresponding author:

Haihong Lv, Department of Endocrinology and Metabolism, The First Hospital of Lanzhou University, 1 Donggang West Road, Lanzhou, Gansu 730000, P.R. China.

Email: haihonglv@126.com



phospholipid structure, and nucleic acid synthesis.¹ The absorption of phosphate is mainly dependent on sodium phosphate cotransporters, of which NaPi-IIa, encoded by *SLC34A1*, is the most important. Mutations of *SLC34A1* lead to NaPi-IIa dysfunction, resulting in phosphate absorption problems and clinical symptoms associated with phosphate deficiency. Clinically, however, hypophosphatemia is rare, and patients with *SLC34A1* mutations often show skeletal abnormalities such as rickets and osteomalacia. Other clinical manifestations include slow growth, a short stature, bone pain, and limb malformation.² Hypophosphatemia is difficult to diagnose and is easily misdiagnosed as osteoporosis, bone tumors, myopathy, and other diseases.

Current treatment of hypophosphatemia mainly involves the supplementation of neutral phosphate. This can be achieved by two methods: oral phosphorus tablets or the dissolving of compound disodium hydrogen phosphate and potassium dihydrogen phosphate in water. Both drugs have been shown to improve hypophosphatemia.³

Here, we present a case of a 38-year-old Chinese woman with pain in multiple bones throughout her body and difficulty with walking for more than 2 years. We obtained her clinical records and carried out genetic analysis of the proband and her family, resulting in a diagnosis of hypophosphatemic kidney stones with osteoporosis. We also explore the pathogenesis and treatment of the disease.

Materials and methods

Ethical approval

The proband and her parents provided their informed consent for participation of the study. This study was approved by the Ethics Committee of the First Hospital of Lanzhou University.

Blood collection and DNA sequencing

A total of 2 mL fasting blood was collected from the proband and her parents between 08:00 and 10:00 hours into ethylenediaminetetraacetic acid-treated tubes. Genomic DNA was extracted using the Blood Genome Column Medium Extraction Kit (Kangweishiji, Beijing, China) according to the manufacturer's instructions. For whole exome library construction, protein-coding exome enrichment was performed using xGen Exome Research Panel v1.0 (Integrated DNA Technologies, Inc., Coralville, IA, USA). This consists of 429,826 individually synthesized and quality-controlled probes, targeting a 39-Mb protein-coding region (19,396 genes) of the human genome and covering 51 Mb of end-to-end tiled probe space. High-throughput sequencing was performed by an Illumina NovaSeq 6000 series sequencer (PE150; Illumina, San Diego, CA, USA), and not less than 99% of the target sequence was sequenced.

Bioinformatics analysis

Raw data were processed by fastp for adapter removal and low-quality read filtering. Variant calling of paired-end reads was performed using the Burrows–Wheeler alignment tool of the Ensembl GRCh37/hg19 reference genome. Base quality score recalibration together with single nucleotide polymorphism (SNP) and short indel calling were conducted using The Genome Analysis Toolkit. SNPs and indels were screened according to the sequence depth and variant quality to obtain high-quality and reliable variants. An online system independently developed by Chigene (www.chigene.org) was used to annotate database-based minor allele frequencies (MAFs), and to determine American College of Medical Genetics (ACMG) practice guideline-based pathogenicity of every yielded gene variant. The system also

provided a serial software package for conservative analysis and protein product structure prediction. Databases for MAF annotation included 1,000 Genomes, dbSNP, ESP, ExAC, and the Chigene in-house MAF database. PROVEAN, SIFT, Polyphen2_hdiv, Polyphen2_hvar, Mutation Taster, M-Cap, and REVEL software packages (database dbNSFP4.0b1a) were used to predict protein product structure variation for the prediction of pathogenicity. As a prioritized pathogenicity annotation to ACMG guidelines, OMIM, HGMD, and ClinVar databases were used as conferences of pathogenicity of every variant. To predict functional changes of variants on splicing sites, MaxEntScan, dbSNV, and GTAG software packages were used instead of product structure prediction software.

Results

Clinical analysis

Two years previously, the patient presented with weakness and pain in her lower limbs, which became progressively aggravated. She has no history of chronic disease such as renal insufficiency, and no long-term use of glucocorticoids or other medication history. Physical examination revealed pain in the bilateral ribs and the muscle strength of both lower limbs was reduced. Her mother suffered a femoral neck fracture from a fall at the age of 45. At the age of 58, her femoral head has now become necrotic so she has undergone surgery.

Biochemical analysis

Biochemical tests of the patient revealed significantly reduced levels of blood phosphorus (AU5800 Clinical Chemistry Analyzer, Beckman Coulter Inc., Brea, CA, USA) ranging from 0.27 to 0.9 mmol/L (normal range, 0.97–1.6 mmol/L), and urinary phosphorus ranged from 9.86 to 19.3 mmol/

24 hours (normal range, 9.7–42.0 mmol/24 hours). However, blood and urinary calcium were normal, and immunoreactive parathyroid hormone levels ranged from 76 to 237 pg/ml (normal range, 11–81 pg/ml). Routine urine tests were also normal. The ratio of the maximum rate of tubular phosphate reabsorption to the glomerular filtration rate ranged from 1.48 to 1.92 mg/dl, indicating a renal phosphate leak (related data are shown in Table 1). Biochemical examination of the proband's mother revealed low serum phosphate, ranging from 0.38 to 0.79 mmol/L. Urinary phosphorus ranged from 8.7 to 18.3 mmol/24 hours, and blood and urinary calcium levels were normal.

Color ultrasound (KR-8288V, Kaier Medical Appliance Co., Ltd., Jiangsu, China) indicated stones in the left kidney of the proband and in the left kidney of her mother. A whole body scan using emission computed tomography (BrightView SPECT; Philips Healthcare, Best, the Netherlands) showed abnormally active bone mineral metabolism in knee, hip, shoulder, and elbow joint areas of the patient, leading to a diagnosis of systemic metabolic bone disease (Figure 1a).

Digital radiography using the Axiom Aristos VX DR (Siemens Healthcare, Erlangen, Germany) exposed cervical bone and lumbar vertebrae hyperplasia, and osteoporosis in the hands and feet of the patient (Figure 1b, 1c). Magnetic resonance imaging using a Magnetom Amira MRI scanner (Siemens Healthcare) revealed a decreased bone signal in the lumbar spine. Dual-energy x-ray absorption with the Lunar iDXA (GE Healthcare, Piscataway, NJ, USA) confirmed osteoporosis in a bone density examination of both the proband (Table 2) and her mother.

DNA sequencing

Whole exon sequencing identified three potentially pathogenic genes: *SLC34A1*, *HRAS*, and *TRH*. *TRH* mutations induce

Table I. The proband's biochemical parameters.

Date	08/23/2016	10/18/2016	09/21/2017	01/16/2018	11/07/2018	11/01/2019
Blood phosphorus (mmol/L)	0.5	0.42	0.3	0.32	0.27	0.9
24 hour urinary phosphorus (mmol/24 hours)	–	11.1	–	9.86	19.3	–
Blood calcium (mmol/L)	2.38	2.30	2.42	2.24	2.33	2.36
24 hour urinary calcium (mmol/24 hours)	–	4.6	–	5.33	7.2	–
iPTH (pg/ml)	76	101.5	101	128.9	237	–

iPTH, immunoreactive parathyroid hormone.

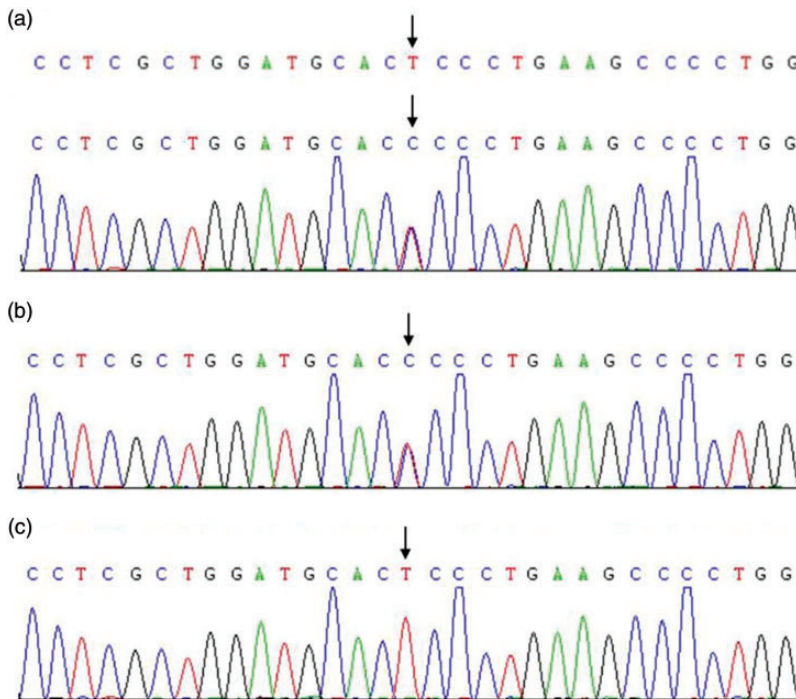


Figure 1. (a) Proband mutation site (c.1753 T>C) in exon 13 of *SLC34A1*. (b) Mutation sites in the mother of the proband (c.1753 T>C). (c) Sequencing of the father of the proband showing wild-type sequence (c.1753 T).

thyrotropin-releasing hormone deficiency syndrome,⁴ which is not related to hypophosphatemia, while *HRAS* mutations cause linear sebaceous nevus syndrome,⁵ which is inconsistent with the clinical manifestations of the proband. Therefore, these

two genes were excluded as pathogenic. Hypophosphatemic kidney stones with osteoporosis caused by *SLC34A1* mutations were consistent with the clinical features of the proband, so mutated *SLC34A1* was considered causative of disease.

Table 2. Bone density analysis of the proband.

Section	Bone mineral density (g/cm ²)	Adults		Compared with healthy individuals of the same age	
		(%)	T-value	(%)	Z- value
L1	.728	71	-2.5	76	-2.0
L2	.784	71	-2.7	76	-2.1
L3	.803	70	-2.9	74	-2.3
L4	.773	68	-3.1	72	-2.5
L1-4	.774	69	-2.8	74	-2.3

**Figure 2.** The mutated amino acid at position 585 (red arrow) is located inside the structural domain of the Phosphate:Na⁺ Symporter Family of proteins according to NCBI/Structure/Cdd.

Sequencing identified a mutation in the 13th exon of *SLC34A1* in the proband: c.1753 T>C. This substitution of a T with a C at position 1753 of *SLC34A1* (Figure 2a) resulted in the replacement of serine by proline at position 585 of the protein (p. S585P). This is a novel mutation that has not been previously reported in the ExAC browser. The proband's mother was also shown to harbor the same mutation (Figure 2b), but the proband's father has the wild-type sequence (Figure 2c).

Computational mutation prediction of the *SLC34A1* conserved domain using the NCBI Conserved Domain Database (Cdd) revealed that the mutated amino acid at position 585 is located inside the structural domain of the Phosphate:Na⁺ Symporter family of transport and binding proteins (Figure 3). Sequence-based mutation

prediction for p. S585P was probably damaging according to NCBI/Structure/Cdd (ncbi.nlm.nih.gov/Structure/cdd/wrpsb.cgi). The mutation was predicted to result in a decrease in phosphate uptake compared with wild-type *SLC34A1*.

Based on the above findings, and combined with the patient's clinical manifestations, she was diagnosed with hypophosphatemic kidney stones with osteoporosis. She was administered 4 mL of 253 g of disodium hydrogen phosphate and 126 g of potassium dihydrogen phosphate dissolved in 1 L water every 5 hours, and calcitriol 0.5 µg/day. After 1 month, her bone pain was relieved, and she was able to walk slowly and independently after more than 2 months. Her blood calcium had normalized after 1 month, and her blood phosphorus level increased to

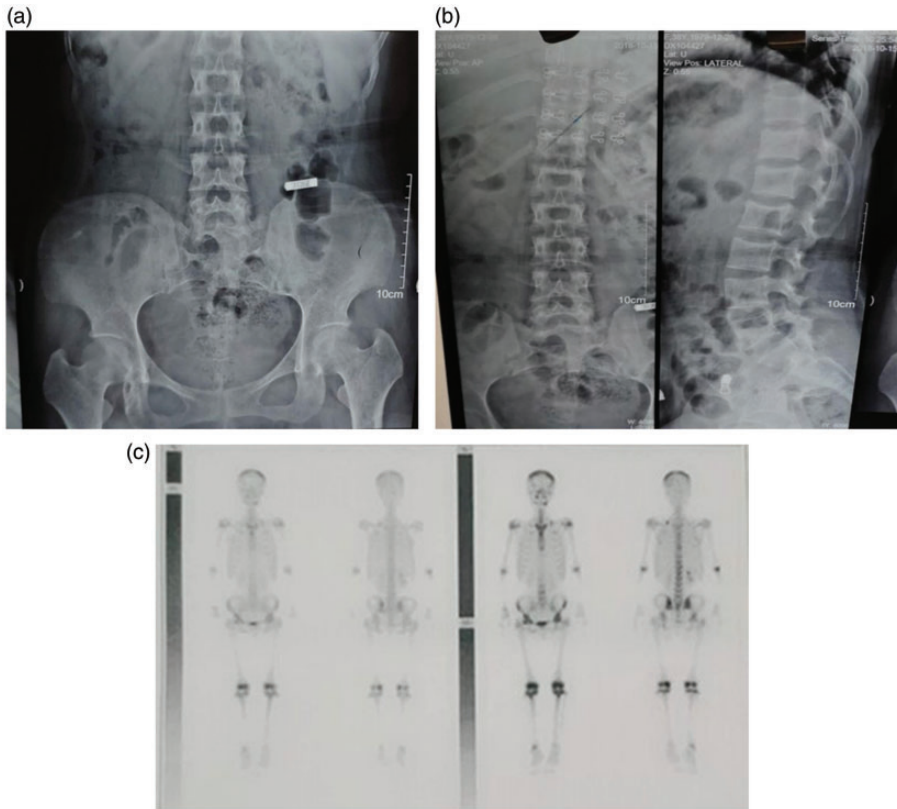


Figure 3. (a) Whole body bone scan emission computed tomography of the patient. (b) Lumbar spine digital radiography of the patient. (c) Pelvis digital radiography of the patient.

0.9 mmol/L after 2 months and normalized after 4 months.

Discussion

Inorganic phosphate plays an important role in bioenergetics, metabolic regulation, intracellular signal transduction, cell proliferation, and the formation of bone and cell membrane structures *in vivo*. Approximately 85% of systemic phosphate accumulates in bones and teeth, 14% in soft tissue, and 1% as free phosphate in extracellular fluid. Phosphorus reabsorbed protein-sodium phosphate cotransporter is divided into three types: NaPi-I, NaPi-II, NaPi-III, encoded by *SLC17*, *SLC34*, and

SLC20, respectively.⁶ Kidney mRNA contents were previously reported to be 15%, 84%, and 1%, respectively, of which NaPi-II was the most important.^{7,8} NaPi-II has three subtypes, NaPi-IIa, NaPi-IIb, and NaPi-IIc which are encoded by *SLC34A1*, *SLC34A2*, and *SLC34A3*, respectively.⁹ NaPi-IIa and NaPi-IIc are localized specifically in the apical brush border membrane of renal proximal tubule cells, whereas NaPi-IIb is found in many tissues, including the luminal brush border membrane of the small intestine and alveolar type II epithelial cells.^{10,11} Studies of knockout mice and human disease have shown the importance of these transporters at the whole body level. Mice lacking NaPi-IIa exhibit

hypophosphatemia and hyperphosphaturia,¹² while those lacking NaPi-IIb die *in utero*.¹³ Human NaPi-IIc mutations cause hereditary hypophosphatemic rickets with hypercalciuria.¹⁴

SLC34A1 is located on chromosome 5q35 and consists of 13 exons and 12 introns.^{11,15} NaPi-IIa consists of 639 amino acids and is mainly expressed on the apical brush border membrane of the proximal tubule of the kidney. *SLC34A1* mutations affect the function of NaPi-IIa, which in turn affects the reabsorption of phosphorus. This indicates that *SLC34A1* is an important determinant of plasma phosphate levels and that it regulates human renal phosphate homeostasis. *SLC34A1* mutations can cause a range of clinical phenotypes, including infant hypercalcemia, proximal renal Fanconi syndrome, and hypophosphatemic kidney stones, all of which are associated with low phosphorus levels. We excluded the first two diagnoses according to the patient's clinical characteristics and test data, so she was ultimately diagnosed with hypophosphatemic kidney stones with osteoporosis.

Our genetic analysis identified the novel mutation c.1753 T>C in exon 13 of *SLC34A1* in the proband and her mother, which results in substitution of serine by proline at position 585 of NaPi-IIa. The mutation was found to be inherited in an autosomal dominant manner. Previous studies showed that cartilage and ligament tissues in the teeth and bones become weakened when the ratio of proline and hydroxyproline is unbalanced, which could be the cause of the clinical manifestations such as bone pain in the proband and her mother. Based on these findings, the proband was diagnosed with hypophosphatemic kidney stones with osteoporosis which was alleviated after the administration of disodium hydrogen phosphate, potassium dihydrogen phosphate, and calcitriol.

In conclusion, hypophosphatemic kidney stones and osteoporosis can be diagnosed by genetic analysis, which would reduce the rate of misdiagnosis. Thus, in cases of systemic bone pain, fractures, and other symptoms and when the examination suggests hypophosphatemia and *SLC34A1* mutation, hypophosphatemic kidney stones and osteoporosis should be considered when there is no notable improvement in symptoms following calcium supplementation.

Acknowledgements

The authors thank the staff of Beijing Chigene Translational Medicine Research Center Co., Ltd., China and the Department of Endocrinology at The First Hospital of Lanzhou University.

Availability of data and materials

The datasets used and/or analyzed during the current study are available from the corresponding author on reasonable request.

Declaration of conflicting interest

The authors declare that there is no conflict of interest.

Funding

This research received no specific grant from any funding agency in the public, commercial, or not-for-profit sectors.

ORCID iD

Haihong Lv  <https://orcid.org/0000-0003-2073-4899>

References

1. Michigami T, Kawai M, Yamazaki M, et al. Phosphate as a signaling molecule and its sensing mechanism. *Physiol Rev* 2018; 98: 2317–2348.
2. Segawa H, Kaneko I, Takahashi A, et al. Growth-related renal type II Na/Pi cotransporter. *J Biol Chem* 2002; 277: 19665–19672.

3. Glorieux FH, Scriver CR, Reade TM, et al. Use of phosphate and vitamin D to prevent dwarfism and rickets in X-linked hypophosphatemia. *New Eng J Med* 1972; 287: 481–487.
4. Katakami H, Kato Y, Inada M, et al. Hypothalamic hypothyroidism due to isolated thyrotropin-releasing hormone (TRH) deficiency. *J Endocrinol Invest* 1984; 7: 231–233.
5. Lim YH, Ovejero D, Sugarman JS, et al. Multilineage somatic activating mutations in HRAS and NRAS cause mosaic cutaneous and skeletal lesions, elevated FGF23 and hypophosphatemia. *Hum Molec Genet* 2014; 23: 145–151.
6. Murer H and Biber J. Phosphate transport in the kidney. *J Nephrol* 2010; 23: 145–151.
7. Beck L, Karaplis AC, Amizuka N, et al. Targeted inactivation of Npt2 in mice leads to severe renal phosphate wasting, hypercalcuri A, and skeletal abnormalities. *Proc Natl Acad Sci U S A* 1998; 95: 5372–5377.
8. Tenenhouse HS, Martel J, Gauthier C, et al. Differential effects of Npt2a gene ablation and X-linked Hyp mutation on renal expression of Npt2c. *Am J Physiol Renal Physiol* 2003; 285: 1271–1278.
9. Forster I, Hernando N, Sorribas V, et al. Phosphate transporters in renal, gastrointestinal, and other tissues. *Adv Chronic Kidney Dis* 2011; 18: 63–76.
10. Traebert M, Hattenhauer O, Murer H, et al. Expression of type II Na-Picotransporter in alveolar type II cells. *Am J Physiol - Lung Cell Mol Physiol* 1999; 277: L868–L873.
11. Wagner CA, Hernando N, Forster IC, et al. The SLC34 family of sodium-dependent phosphate transporters. *Pflugers Arch* 2014; 466: 139–153.
12. Beck L, Karaplis AC, Amizuka N, et al. Targeted inactivation of Npt2 in mice leads to severe renal phosphate wasting, hypercalciuria, and skeletal abnormalities. *Proc Natl Acad Sci USA* 1998; 95: 5372–5377.
13. Shibasaki Y, Etoh N, Hayasaka M et al. Targeted deletion of the tybe Iib Na+-dependent Pi-co-transporter, NaPi-Iib, results in early embryonic lethality. *Biochem Biophys Res Commun* 2009; 381: 482–486.
14. Bergwitz L, Roslin NM, Tieder M, et al. SLC34A3 mutations in patients with hereditary hypophosphatemic rickets with hypercalciuria predict a key role for the sodium-phosphate cotransporter NaPi-IIc in maintaining phosphate homeostasis. *Am J Hum Genet* 2009; 78: 179–192.
15. Hartmann CM, Hewson AS, Kos CH, et al. Structure of murine and human renal type II Na + -phosphate cotransporter genes (Npt2 and NPT2). *Proc Natl Acad Sci U S A* 1996; 93: 7409–7414.